

## An Improved 2D-FDTD Algorithm for Hybrid Mode Analysis of Quasi-planar Transmission Lines

S.Xiao and R.Vahldieck

*Laboratory for Lightwave Electronics, Microwave and Communications*

*(LLiMiC)*

*Department of Electrical and Computer Engineering*

*University of Victoria*

*Victoria, B.C., Canada, V8W 3P6*

### Abstract

A significantly improved two-dimensional finite difference time domain (FDTD) method is proposed for the full-wave analysis of guided wave structures. By using a phase shift  $\beta\Delta z$  along the z-direction (propagation direction), and assuming the limiting case of  $\Delta z$ , the propagation constant of hybrid modes can be calculated by using a two-dimensional mesh with a truly two-dimensional grid size. Secondly, by appropriately arranging variables, only a real impulse response is involved. Furthermore, a new grading scheme is introduced allowing a gradually non-equidistant mesh in three dimension.

### Introduction

Memory space requirements and computational efficiency are major problems in the use of the FDTD method. To alleviate some of the problem, a modified FDTD approach was introduced recently [1-4]. In this approach only a two-dimensional mesh consisting of a 3D space grid along the z-direction was necessary for hybrid mode analysis of guided wave structures. This mesh could also be regard as one slice out of a 3D mesh, with the third dimension, the propagation direction, being replaced by introducing a phase shift  $\beta\Delta z$ . The resultant space grid was only half of its normal size (Fig.1a). As a result, the convergence rate was much faster than in the conventional (3D FDTD) approach and the required memory space was also reduced significantly. Subsequently, other authors followed this idea [4-7].

To take our approach one step further, in this paper we propose to reduce the mesh size in propagation direction to the limiting case of zero. This results in a truly 2-D grid as shown in Fig. 1b and a significantly improved convergence rate. Furthermore, due to an appropriate coordinate transformation, we are able to achieve a real impulse response, which is a

significant improvement of our original approach, because now all variable used in the computation are real instead of complex numbers. This makes the algorithm computationally very efficient.

Furthermore, we introduce a new scheme which allows us to use a graded mesh in 3 dimensions and maintaining a second order accuracy. This feature is very attractive for the FDTD method because a non-uniform mesh allows the resolution of highly localized fields at circuit corners without reducing the accuracy of the scheme. A number of papers have been published before on this subject, such as [8] and [9]. The major problem was always that changing the size of neighboring lattices continuously and simultaneously (with arbitrary mesh ratios) in all three space directions introduces a first order error term [10]. To overcome this problem, this paper introduces two techniques in which the second order accuracy can be maintained. One method uses a special mesh arrangement (valid only for certain mesh ratios) without changing the algorithm for the uniform mesh arrangement. The other method uses a universal grading scheme with continuously variable lattice size in all three space dimensions.

### Theory

As shown in [3, 4], a phase shift  $\exp\{-j\beta z\}$  is involved at any adjacent nodes for any specific propagation constant  $\beta$ . This modal knowledge is used to simplify the scheme. It is easy to see that any incident or reflected impulse for any propagation constant  $\beta$  satisfies

$$E_x^n, E_y^n, H_z^n = \{E_x^n(x, y), E_y^n(x, y), H_z^n(x, y)\} j \exp\{j\beta z\} \quad (1a)$$

$$H_x^n, H_y^n, E_z^n = \{H_x^n(x, y), H_y^n(x, y), E_z^n(x, y)\} \exp\{j\beta z\} \quad (1b)$$

Where the factor  $j$  in (1a) is introduced in order to obtain a real-variable impulse process. The value of this step will become apparent in the following. In [3] and [4] it was assumed that the discretization size  $\Delta z$  in the propagation direction was of finite value. This led to the half grid size shown in Fig. 1a and (5) in [3].

However it is not necessary to keep  $\Delta z$  finite. Instead, when  $\Delta z$  approaches zero, the limiting case for the discretized Maxwell's equations for x-direction field components yields:

$$\begin{aligned} H_x^{n+0.5}(i, j) &= H_x^{n-0.5}(i, j) - \frac{\Delta t}{\mu} [(E_z^n(i, j+1) - E_z^n(i, j)) / \Delta y - \beta E_y^n(i, j)] \\ E_x^{n+1}(i, j) &= E_x^n(i, j) + \frac{\Delta t}{\epsilon} [(H_z^{n+0.5}(i, j+1) - H_z^{n+0.5}(i, j)) / \Delta y \\ &\quad + \beta H_y^{n+0.5}(i, j+1)] \end{aligned} \quad (2)$$

Where  $\Delta t$ ,  $\Delta x$ , and  $\Delta y$  are, respectively, the time step and the space steps in the x- and y-direction. The central finite difference scheme has been used to discretize the space along the x- and y-directions as well as the time axis t.

From the above equations, it is obvious that now only a two-dimensional process is involved with a truly 2-D grid size as shown in Fig.1b. Another important point here is that now all quantities in (2) are real numbers because of the variable transformation by a factor of j in (1). The condition of stability of the new scheme is found to be

$$v_p \Delta t \leq 1 / \sqrt{\Delta x^{-2} + \Delta y^{-2}} \quad (3)$$

### Graded Lattice

The problem of first order error in the variable lattice scheme can be illustrated by looking into the expression for the  $E_x$ -field at the boundary for two neighboring lattices as an example:

$$E_x^n(i, j, k) = E_x^n(i, j, k) + \frac{\Delta t}{\epsilon_x} \left[ \frac{\partial H_z^{n+0.5}(i, j, k)}{\partial x} - \frac{\partial H_y^{n+0.5}(i, j, k)}{\partial z} \right] \quad (4)$$

Developing the x-dependent term in this equation by a Taylor series yields:

$$\begin{aligned} \frac{\partial H_z^{n+0.5}(i, j, k)}{\partial x} &= \frac{H_z^{n+0.5}(i, j+1, k) - H_z^{n+0.5}(i, j, k)}{\Delta h(q_j + q_{j+1})/2} \\ &\quad + o((q_{j+1} - q_j)\Delta h) \end{aligned} \quad (5)$$

which clearly shows that normally a variable grading scheme provides only first order accuracy.

To obtain second order accuracy without changing the uniform FDTD scheme the lattices have to be arranged in a certain ratio. Without loss of generality, let us first consider only the one dimensional case as an example, shown in Fig.2. The FDTD algorithm on the left and right side of point D in Fig. 2 obviously keeps a second order accuracy since the central finite differences are maintained. The problem is that calculating the electric field component at point D from the magnetic field components at points C and E inevitably leads to a first order accuracy because central finite differences are not maintained. This follows also from equ. (5). But, interestingly enough, a second order accuracy can be obtained if the magnetic

field components at point A and E are used for the calculation of the electric field component at point D instead of the magnetic field components at point C and E. An appropriate mesh ratio between left and right sides is used (Fig. 2) in order to cancel the first order errors. The points A, C, and E are so chosen that the point D is in the middle of point C and point E. This means that the neighboring mesh ratios are selected as  $r=3:1$ . The advantage of this improvement is that it does not change the uniform mesh algorithm. The limitation of this scheme is that an appropriate mesh ratio must be satisfied to obtain the central finite differences. Other examples for lattice size ratios which can be realized are  $r=1:5=0.2$ ,  $1/r=3:5$ , and,  $1/r=7:5=1.4$ , respectively.

For non-integer lattice ratios the second order error can only be obtained by combining the three neighboring lattice cells. Considering an arbitrary variable lattice as shown in Fig. 3, the mesh parameters  $p_i$  ( $i=1,2,\dots,M$ ),  $q_j$  ( $j=1,2,\dots,N$ ), and  $r_k$  ( $k=1,2,\dots,K$ ) are any positive real numbers as required to resolve the specific structure.  $s=c\Delta t/\Delta h$ ,  $\Delta t$  and  $\Delta h$  are, respectively, the time and the space steps. If  $p_i=\text{constant}$  ( $i=1,2,\dots,M$ ),  $q_j=\text{constant}$  ( $j=1,2,\dots,N$ ) and  $r_k=\text{constant}$  ( $k=1,2,\dots,K$ ), the variable lattice will be reduced to a cubic one. If all mesh parameters along the x-, y-, and z-direction are set to unity, the lattice will be a uniform cube. Once again, the one dimensional case is treated as an example without loss of generality. The three dimensional case may be easily derived from the one-dimensional case. The electric field components can be always arranged in the middle of the magnetic field components or vice versa. Therefore, calculating the electric (or magnetic) field components from the magnetic (or electric) field components leads to a second order accuracy since a central finite difference is maintained. However, on the boundary between the variable grading lattices the E-field (point D in Fig.2) is not located exactly in the middle between C and E and therefore calculating the E-field from the H-field leads to a first order error. This again follows from equ.(5). The important thing is that a compensation factor can always be found to cancel the first order error terms and therefore a second order accuracy can be obtained. This is demonstrated in the following.

If we use the central finite difference schemes to calculate the electric field components from the magnetic field components, it is obvious that the electric field components are at the electric field nodes shown in Fig. 3, and a Taylor's series analysis yields

$$E_y(i) = E_y^A(i) + \Delta \frac{\partial E_y^A(i)}{\partial x} + o(h^2) \quad (6)$$

The first order partial differential term in the above equations may be expressed by using the first order partial differential expansion at the electric nodes as follows

$$\frac{\partial E_y^A(i)}{\partial x} = \frac{\partial E_y(i)}{\partial x} + \delta_i \frac{\partial^2 E_y(i)}{\partial x^2} + o(h^2) \quad (7)$$

and therefore, equ. (6) can be written as

$$E_y(i) = E_y^A(i) + \Delta_i \left[ \frac{E_y(i+1) - E_y(i-1)}{l^i} \right] + o(h^2) \quad (8)$$

where,  $l_i$  ( $i=1, 2, \dots, N$ ) is time independent and fixed for a specific mesh arrangement. The compensation terms in the bracket of the right side of the equ.(8) have been calculated in the neighboring equations and therefore the new algorithm requires not much more computations. From equ. (8), it is clear that a variable mesh scheme with arbitrary lattice ratio and a second order accuracy is feasible by combining neighboring mesh field components. Similarly for other field components, a second order accuracy may be obtained through a compensation factor. This idea can be extended to all three dimensions.

### Numerical Result

To compare the accuracy of the new scheme with results obtained from other methods, the following comparison is made. Fig. 4 shows the dispersion diagram for a unilateral finline in comparison with results obtained from the method of lines (MoL) and the modified FDTD. Fig. 5 and Fig. 6 demonstrate the frequency dependent dielectric constant of a multiconductor stripline and a suspended substrate coplanar line, respectively, in comparison with [13] and [12]. The CPU-time required is from a few seconds to a few minutes, depending on the structure, on a SPARC II workstation.

Fig. 7 shows the return loss for a low-pass filter analyzed with the variable lattice method introduced in this paper. A comparison between experimental results, uniform lattice size and variable lattice sizes with ratio  $1/r=3:1$  and  $r=1:2$  is given in this figure. The uniform mesh layout requires  $160 \times 100 \times 32$  cells with  $\Delta x=0.2032\text{mm}$ ,  $\Delta y=0.4233\text{mm}$  and  $\Delta z=0.265\text{mm}$ . The computation time on a IBM Risk 6000 is around 4 hours. The variable mesh with ratio 1:2 starting from the metal edges required a CPU-time of 20 minutes, while the ratio of 1:3 required a CPU-time of 18 minutes. The ratio of 1:2 utilized  $100 \times 92 \times 10$  cells. In terms of the accuracy, the uniform mesh ratio and the ratio of 1:2 provided the best comparison to the measured data. However, the latter one was much faster and consumed much less memory.

### Conclusion

A 2-D full-wave FDTD algorithm with only a real impulse response has been introduced. Using a truly 2-D grid the memory space and CPU-time of the FDTD has been further reduced. For 3D analysis in the time and frequency-domain a new variable mesh techniques has been introduced to enhance the FDTD efficiency significantly. Measured and computed results have shown excellent agreement.

### Reference

- [1] H. Jin, R. Vahldieck and S. Xiao, "A full-wave analysis of arbitrary guiding structure using 2-D TLM mesh", *21th European Microwave Conference Digest*, pp.205-210, German, Sept., 1991.
- [2] H. Jin, R. Vahldieck and S. Xiao, "An improved TLM full-wave analysis using two dimensional mesh", *1991 IEEE MTT-S International Microwave Symposium Digest*, pp.675-677, Boston, MA, Jun. 1991.
- [3] S.Xiao, R.Vahldieck, and H.Jin, "A fast 2-D FDTD full wave analyzer for arbitrary guided wave structures," *IEEE Guided Wave Letters*, pp.165-167, May 1992.
- [4] S.Xiao, R.Vahldieck, H.Jin, "A fast 2-D FDTD full-wave analyzer with an adaptive mesh size," *1992 IEEE-S International Microwave Symposium Digest*, Albuquerque, NM, Jun. 1992.
- [5] A. Asi and L. Shafai, "Dispersion analysis of anisotropic inhomogeneous waveguides using compact 2D-FDTD", *Electronics Letters*, pp.1450-1451, vol.28, July, 1992.
- [6] F.Arndt, V.J.Brankovic and D.V.Kruzevic, "An improved FD-TD full wave analysis for arbitrary guiding structures using a two dimensional mesh", *1992 IEEE MTT-S International Microwave Symposium Digest*, Jun. 1992.
- [7] A.C.Cangellaris, "Numerical stability and numerical dispersion of a compact 2-D/FDTD method used for the dispersion analysis of waveguides", *IEEE Guided Wave Letters*, Dec. 1992.
- [8] D.H.Chi and W.F.R.Hoefer, "A graded mesh FDTD algorithm for eigenvalue problems", pp.413-417, *17th European microwave conference Digest*, 1987.
- [9] S.S.Zivanovic, K.S.Yee, and K.K.Meit, "A subgridding method for the FDTD method to solve Maxwell's equations," *IEEE Trans. Microwave Theory Tech.*, vol.MTT-39, No.3, pp.471-479, 1991.
- [10] D.L.Paul, E.M.Daniel, C.J.Railton, "Fast finite difference time domain method for the analysis of planar microstrip circuits", pp.303-308, *21th European Microwave Conference Digest*, German, Sept., 1991.
- [11] D.M.Sheen, S.M.Ali, M.D.Abuzahe, J.A.Kong, "Application of the 3-D FDTD to the analysis of planar microstrip circuits", *IEEE Trans. Microwave Theory Tech.*, vol.38, pp.849-857, 1990.
- [12] F.Alessandri, U.Goebel, F.Melai, R.Sorrentino, "Theoretical and experimental characterization of nonsymmetrically shielded coplanar waveguides for millimeter-wave circuits", *IEEE Trans. Microwave Theory Tech.*, pp.2020-2027, vol.MTT-37, no.12, Dec.1989.
- [13] J.J.Yang, G.E.Howard, Y.L.Chow, "A simple technique for calculating the propagation dispersion of multiconductor transmission lines in multilayer dielectric media", *IEEE Trans. Microwave Theory Tech.*, pp.622-627, vol.MTT-40, no.4, April.1992.

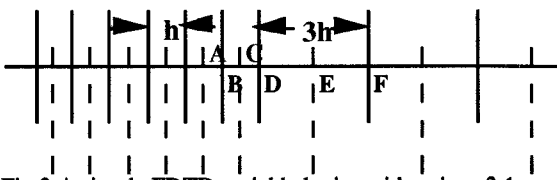


Fig.2 A simple FDTD variable lattice with ratio  $r=3:1$ .

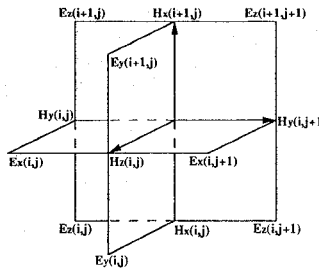


Fig.1a A novel 2-D FDTD mesh

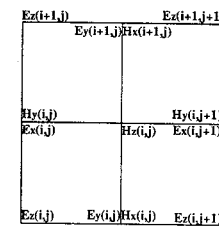


Fig.1b A modified FDTD mesh with a truly 2-D grid.

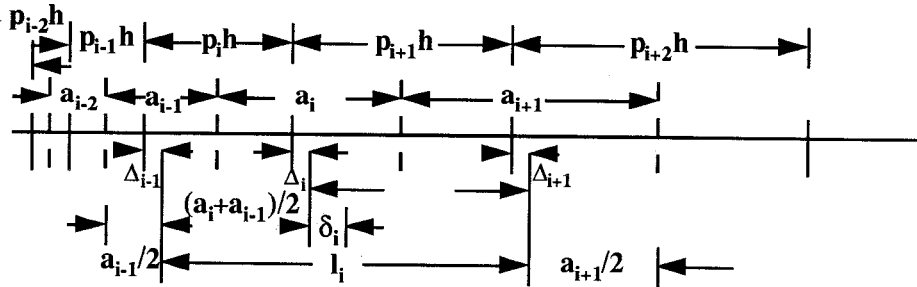


Fig.3 A universal grading lattice

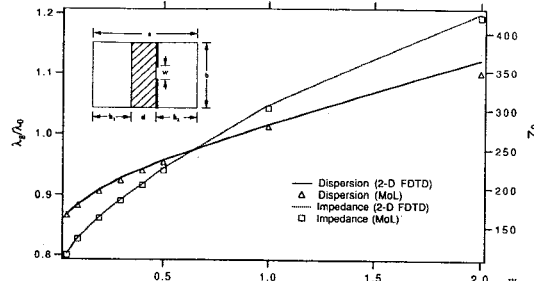


Fig.4 Modified FDTD results compared with the MoL and FDTD for a finline, WR-28 waveguide,  $h_2=3.556$  mm,  $d=0.254$  mm,  $\epsilon_r=2.22$ ,  $f=34$  GHz.

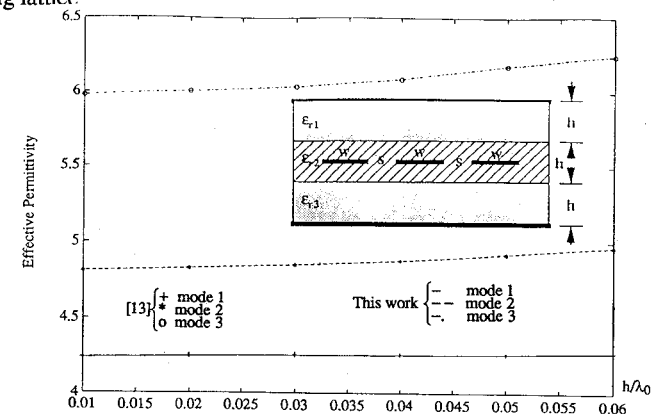


Fig.5 Effective dielectric constant of a three-conductor stripline versus  $h/\lambda_0$ ,  $\epsilon_{r1}=\epsilon_{r3}=9.7$ ,  $\epsilon_{r2}=4.0$ ,  $w/h=1.0$ ,  $s/h=0.1$  [13].

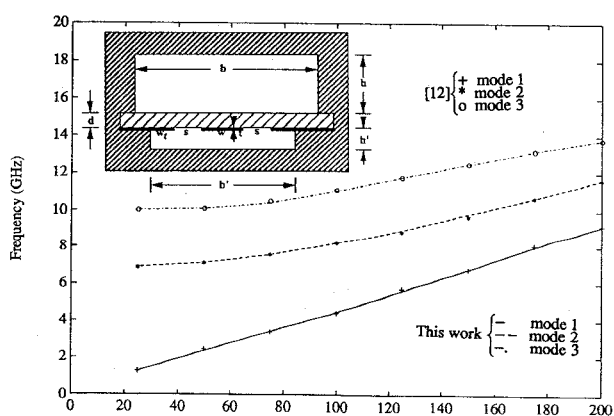


Fig.6 Dispersion in a shielded CPW analyzed by the FDTD and [12],  $\epsilon_r=3.75$ ,  $b=2h=3.22$  mm,  $b'=2.22$  mm,  $h'=0.805$ ,  $d=0.154$  mm,  $t=0.005$ .

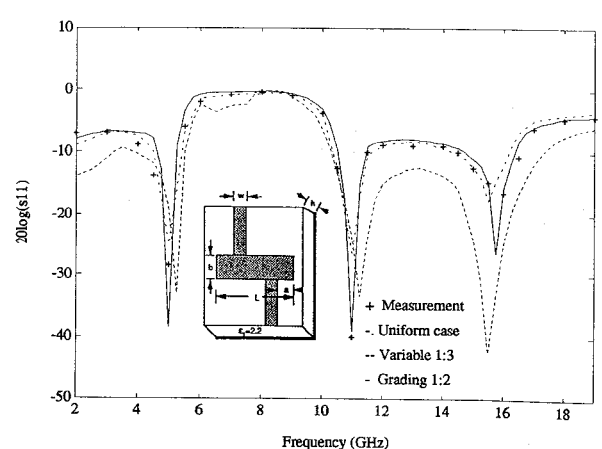


Fig.7 Numerical results of various grading schemes compared to measurements;  $b=2.54$  mm,  $w=2.413$  mm,  $h=0.794$  mm,  $a=5.65$  mm,  $L=20.32$  mm.